

# Enhanced Catalytic Activity through the Tuning of Micropore Environment and Supercritical CO<sub>2</sub> Processing: Al(Porphyrin)-Based Porous Organic Polymers for the Degradation of a Nerve Agent Simulant

Ryan K. Totten, Ye-Seong Kim, Mitchell H. Weston, Omar K. Farha,\* Joseph T. Hupp,\* and SonBinh T. Nguyen\*

Department of Chemistry and the International Institute for Nanotechnology, Northwestern University, 2145 Sheridan Road, Evanston, Illinois 60208-3113, United States

**S** Supporting Information

**ABSTRACT:** An Al(porphyrin) functionalized with a large axial ligand was incorporated into a porous organic polymer (POP) using a cobalt-catalyzed acetylene trimerization strategy. Removal of the axial ligand afforded a microporous POP that is catalytically active in the methanolysis of a nerve agent simulant. Supercritical CO<sub>2</sub> processing of the POP dramatically increased the pore size and volume, allowing for significantly higher catalytic activities.

Over the past decade, much efforts have been made to heterogenize homogeneous catalysts by integrating them into microporous materials, such as metal-organic frameworks (MOFs),<sup>1–5</sup> covalent organic frameworks (COFs),<sup>6,7</sup> polymers of intrinsic microporosity (PIMs),<sup>8,9</sup> conjugated microporous polymers (CMPs),<sup>10,11</sup> and porous organic polymers (POPs).<sup>12,13</sup> Beyond the obvious advantages of site isolation<sup>14,15</sup> and recyclability,<sup>4,13,16</sup> this type of incorporation allows for the “close packing” of multiple active metal sites into a porous environment that can be used synergistically to bind and preconcentrate substrates for catalysis.<sup>1</sup> Additionally, nondirective interactions, such as van der Waals forces and solvophobic effects, can be used to further enhance the encapsulation of substrates inside the micropores for catalytic transformations.<sup>17–19</sup> With these advantages, reactions catalyzed by microporous materials can begin to mimic those catalyzed by biological or supramolecular analogues.

Recently, we demonstrated the catalytic activity of homogeneous supramolecular Al(porphyrin) dimers<sup>18</sup> and tetramers<sup>19</sup> in the methanolytic degradation of *p*-nitrophenyl diphenyl phosphate (PNPDPP), a common simulant for toxic nerve agents.<sup>20</sup> The most critical factors for observing enhanced catalysis rates in these systems over that of the corresponding monomers are the optimal positioning of Lewis acidic Al(porphyrin) metal sites, one of which binds and activates an organophosphate substrate so that a nearby second site can deliver a methoxide nucleophile to the phosphorus center in a cooperative fashion. The hydrophobic environment of the porphyrinic cavity further enhances catalysis by solvophobically attracting the relatively hydrophobic PNPDPP substrate in polar methanol. In an effort to heterogenize this biomimetic

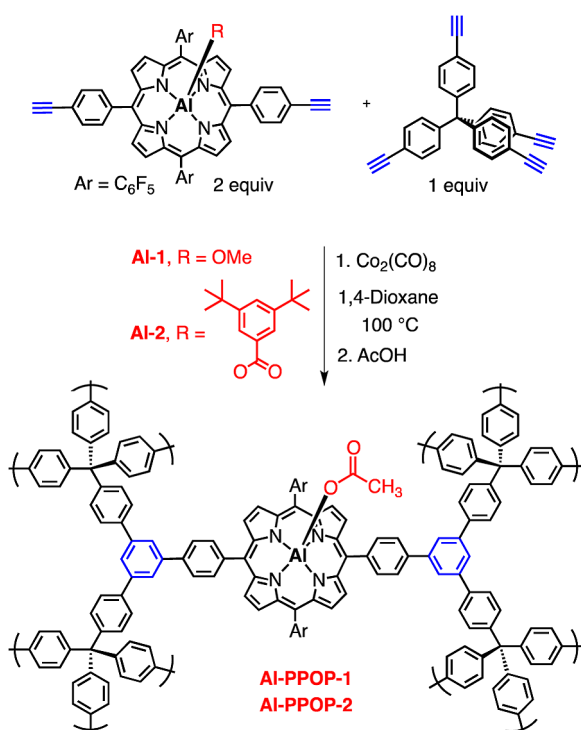
catalyst design,<sup>18</sup> we reasoned that an all-organic Al(porphyrin)-based POP (Al-PPOP) with the right pore environment could mimic the aforementioned characteristics while offering the additional advantages of recyclability and enhanced catalysis rates based on preconcentration. Herein, we report the synthesis of an Al(porphyrin)-based POP (Scheme 1) capable of catalyzing the methanolytic degradation of PNPDPP. Its catalytic activity can be enhanced by over 1 order of magnitude through a combination of tuning the micropore environment and supercritical CO<sub>2</sub> processing.

In designing catalytically active Al-PPOPs, we wanted to control, through the incorporation of rigid spacers, the micropore environment and thus the ability to encapsulate organophosphate substrates for catalysis. For our Al(porphyrin) supramolecular dimers<sup>18</sup> and tetramers,<sup>19</sup> the selection of a proper template to control the cavity shape and size of the resulting assemblies is quite important. While the spacing of Al(porphyrins) within a highly cross-linked polymer network, such as a POP, is significantly influenced by the choice of the “crosslinking” nodes,<sup>8,21,22</sup> we hypothesized that temporarily complexing a large axial ligand to the Al<sup>III</sup> metal center could further displace porphyrin monomers during the polymerization process to afford materials with larger and more accessible pores, capable of effecting the catalysis of large substrates such as PNPDPP. To test this strategy, we compare Al-PPOPs made from each of two Al(porphyrins): one possessing a small methoxide axial ligand and the other possessing a much larger 3,5 di-*t*-butyl benzoate ligand.

For the POP synthesis, we chose a cobalt-catalyzed acetylene trimerization strategy<sup>23,24</sup> given its lack of reactants or side products (i.e., protonated species) that may compete with the axial ligand of the Al(porphyrin) during polymerization. The copolymerization of a *T<sub>d</sub>*-directing *tetrakis*(4-ethynylphenyl)-methane monomer with either one of two Al(porphyrin) monomers (Al-1, R = OMe; Al-2, R = 3,5 di-*t*-butyl benzoate; Scheme 1) proceeded smoothly in the presence of Co<sub>2</sub>(CO)<sub>8</sub> to afford the desired POPs in good yields as deep-purple solids. Subsequent thermal treatment (100 °C) in excess acetic acid to remove the cobalt and the initial axial ligands (see SI, section

Received: June 1, 2013

Published: July 22, 2013

Scheme 1. Synthesis of Al-PPOPs via a Cobalt-Catalyzed Acetylene Trimerization<sup>a</sup>

<sup>a</sup>PPOPs shown above are idealized representations of a completely formed network. However, different substitution patterns (1,3,4 vs 1,3,5) may be present, as well as terminal olefins/dienes and unreacted acetylene groups due to incomplete polymerization. Solid-state <sup>1</sup>H-<sup>13</sup>C CP-MAS NMR analyses of the Al-PPOP compositions shown above suggested that these contain significant amounts of olefin/diene groups (see SI, Figures S5 and S6).

S4), results in two acetate-substituted Al(porphyrin) POPs, Al-PPOP-1 and Al-PPOP-2, with N<sub>2</sub>-derived BET surface areas of 640 and 660 m<sup>2</sup>/g, respectively, upon activation at 150 °C.

Although both Al-PPOP-1 and Al-PPOP-2 exhibit similar surface areas, their pore size distributions reveal distinct differences in dominant pore size: Al-PPOP-2 has two dominant pores at 9 and 12.5 Å, while Al-PPOP-1 has only one dominant pore at 9 Å. This difference is clearly reflected in their catalytic activities in the methanolysis of PNPDP (Table 1), with Al-PPOP-2 being 65% faster than Al-PPOP-1, accentuating the important role that the larger pore plays in the catalysis by Al-PPOP-2. Together with previous

**Table 1. Observed Initial Rates in the Methanolysis of PNPDP by Al-PPOPs**

catalyst <sup>a</sup>	BET surface area (m <sup>2</sup> /g)	observed initial rate (M/s) <sup>b</sup>	relative rate vs uncat reaction
Al-PPOP-1	640	2.8 × 10 <sup>-7</sup>	17
Al-PPOP-2	660	4.8 × 10 <sup>-7</sup>	28

<sup>a</sup>Reaction conditions: PNPDP (25 mM), [Al<sup>III</sup>] (1 mM, 4 mol %), MeOH, 60 °C. <sup>b</sup>Initial rates were measured up to 10% conversion and corrected against background reactions.

reports,<sup>5,12,25–27</sup> this observation demonstrates that specific surface area is not always an accurate indicator of catalytic activity in microporous materials. Rather, the ability to access the catalytic site via larger pores is more influential on the catalytic rate.

Encouraged by the significant improvement of catalysis rate in Al-PPOP-2, we suspected that further enhancement would be possible if the accessibility of catalyst sites inside the pores can be further improved. To this end, we reasoned that the larger pores in POPs, particularly “interparticle” mesopores,<sup>28</sup> could be collapsing upon solvent removal at 150 °C under vacuum, and thus limiting access of substrates to catalytic sites. That is, forced solvent removal via conventional, thermal activation may engender aggregation of POP particles, thereby inhibiting reactant access to some catalyst sites. This hypothesis is prompted by the observation that the syntheses of our Al-PPOPs afforded gel-like materials that initially filled the entire reaction volume (see SI, Figure S24) but then shrunk significantly upon work up. This is akin to the observed collapse of aerogels under fast solvent evaporation where strong capillary forces cause shrinkage and ultimate collapse of mesopores.<sup>29</sup> A similar line of reasoning has been proposed to explain why supercritical CO<sub>2</sub> processing has greatly improved the surface areas of organic-containing microporous materials, such as MOFs,<sup>28</sup> to achieve some of the highest reported surface areas to date.<sup>30–32</sup>

To test the aforementioned hypothesis, we resynthesized Al-PPOP-2 and activated the as-synthesized gel-like materials using supercritical CO<sub>2</sub> processing. To our pleasant surprise, the surface area of the supercritically processed sample, <sup>sc</sup>Al-PPOP-2, increased from 660 to 950 m<sup>2</sup>/g compared to the thermally activated sample. Remarkably, the isotherm for <sup>sc</sup>Al-PPOP-2 changed to a Type II (Figure 1b), indicating a gain in mesoporosity (pore sizes between 20 and 50 Å), along with a 3-

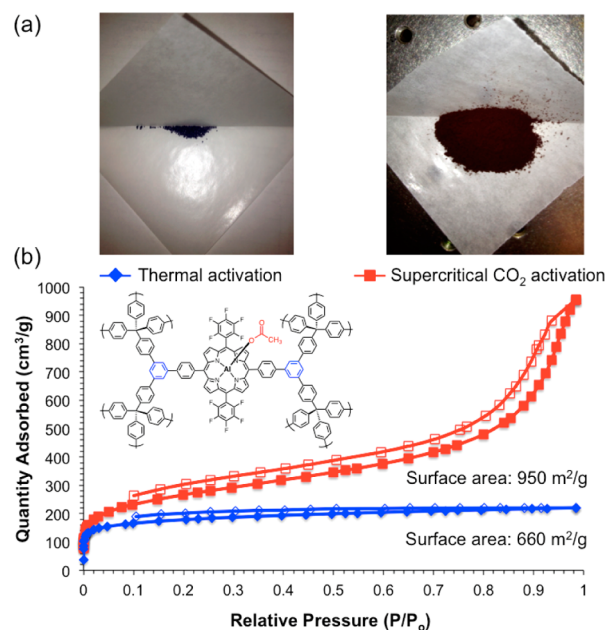


**Figure 1.** (a) Photographic images of Al-PPOP samples (50 mg each) that were either activated thermally (left) or processed with supercritical CO<sub>2</sub>. (b) N<sub>2</sub> isotherms measured at 77 K of Al-PPOP-2 (blue diamonds) and <sup>sc</sup>Al-PPOP-2 (red squares). Closed symbols, adsorption; open symbols, desorption.

fold increase in total pore volume from 0.34 to 1.15 cm<sup>3</sup>/g. Indeed, its BET-derived pore size distribution shows dominant pore sizes of 12, 15, and 18 Å, in addition to a broad mesopore population that centers around 27 Å (see SI, section S12). As a result, the bulk density of <sup>sc</sup>PAl-PPOP-2 (0.53 g/cm<sup>3</sup>) is much less than that of Al-PPOP-2 (0.98 g/cm<sup>3</sup>, see SI, section S16). These differences are accompanied by a drastic change in physical appearance, as <sup>sc</sup>PAl-PPOP-2 is significantly more “powdery” and flocculent than Al-PPOP-2, which is more “chunky,” dense, and brittle (Figure 1a). Together, these data suggest that catalyst sites within supercritically processed Al-PPOPs should be much more accessible to substrates in the methanolytic degradation of organophosphate esters.

Consistent with our hypothesis, the methanolysis of PNPDP is significantly enhanced by the supercritical CO<sub>2</sub> processed Al-PPOPs compared to the thermally activated Al-PPOPs. With a half-life of 90 min, the rate of PNPDP methanolysis by <sup>sc</sup>PAl-PPOP-2 is 7 times that of Al-PPOP-2 and ~200-fold greater than that of the uncatalyzed reaction (Figure 2, see also Table 2).<sup>33</sup> That the rate of PNPDP

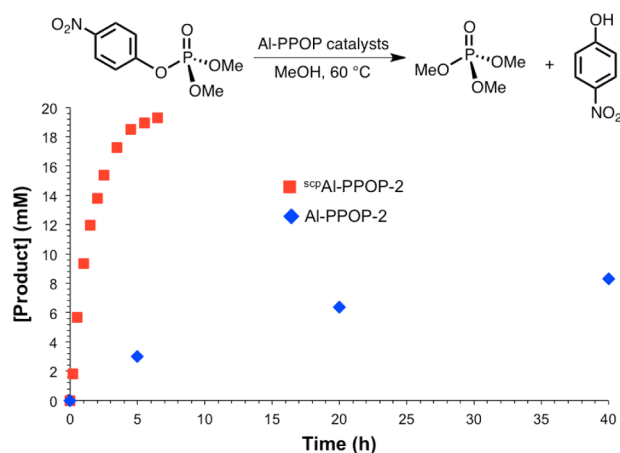


**Figure 2.** Reaction profiles for the methanolysis of PNPDP in the presence of 4 mol % of Al-PPOP-2 (blue diamonds) and <sup>sc</sup>PAl-PPOP-2 (red squares).

**Table 2.** Pore, Surface, and Catalytic Properties of Al(porphyrin)-Based POPs

catalyst <sup>a</sup>	BET surface area (m <sup>2</sup> /g)	total NLDFT-derived pore volume (cm <sup>3</sup> /g) <sup>b</sup>	dominant pore diameter (Å)	observed initial rate (M/s) <sup>c</sup>	relative rate vs uncat reaction
Al-PPOP-1	640	0.35	9	2.8 × 10 <sup>-7</sup>	17
Al-PPOP-2	660	0.34	9, 12.5	4.8 × 10 <sup>-7</sup>	28
<sup>sc</sup> PAl-PPOP-1	830	1.02	12, 15, 18, 27	1.5 × 10 <sup>-6</sup>	88
<sup>sc</sup> PAl-PPOP-2	950	1.15	12, 15, 18, 27	3.5 × 10 <sup>-6</sup>	205

<sup>a</sup>Reaction conditions: PNPDP (25 mM), [Al<sup>III</sup>] (1 mM, 4 mol %), MeOH, 60 °C. <sup>b</sup>Total NLDFT-derived pore volume from the N<sub>2</sub> adsorption profiles at p/p<sub>0</sub> = 0.98. <sup>c</sup>Initial rates were measured up to 10% conversion and corrected against background reactions.

methanolysis by <sup>sc</sup>PAl-PPOP-2 is 2-fold faster than that for <sup>sc</sup>PAl-PPOP-1 again reinforces the aforementioned advantage of templating, where the use of a large axial spacer can lead to better catalytic activity. Although the supercritical CO<sub>2</sub>

processed Al-PPOPs are significantly more “powdery” and have larger surface areas than the thermally activated Al-PPOPs (Figure 1a), the most important factors for enhanced catalysis appear to be larger pore volumes and the presence of mesopores that make catalyst sites more accessible to the PNPDP substrate for solvolysis: a finely ground sample of thermally activated Al-PPOP-2 elicits only a 1.4-fold increase in initial rate over the unground sample (see SI, section S7).

Surprisingly, the initial PNPDP methanolysis rate of <sup>sc</sup>PAl-PPOP-2 drops by 10-fold when it is reused (see SI, Figure S10). Upon closer examination of the reaction profile for the second cycle, we observed a 30 min induction period, which suggests that substrates/products were retained within the pores and blocked new substrates from entering (see SI, Figure S11).<sup>27</sup> To remedy this problem, we Soxhlet-extracted the catalyst with methanol after the first cycle (see SI, section S9). Although a significant amount of the entrapped material was observed and the induction period was eliminated, the catalytic activity of the Soxhlet-extracted material was not restored. This led us to an alternate hypothesis that the loss of mesoporosity, engendered by POP aggregation, could have occurred during the catalysis, causing the reduction in activity. Thus, we reprocessed the <sup>sc</sup>PAl-PPOP-2 sample with supercritical CO<sub>2</sub> after the first cycle and reused it for PNPDP methanolysis. Remarkably, the catalytic activity of <sup>sc</sup>PAl-PPOP-2 was almost fully restored to its initial level (see SI, section S10). Furthermore, the BET surface area and pore size distributions of this recycled, supercritical-CO<sub>2</sub>-processed material were similar to the as-synthesized <sup>sc</sup>PAl-PPOP-2 sample (see SI, sections S13 and S14), further demonstrating the importance of mesoporosity in enhancing the accessibility of catalyst sites.

In summary, we have demonstrated that catalytically active Al(porphyrin) moieties can be integrated into an all-organic porous network for use in the methanolytic degradation of a nerve agent simulant. While the presence of a large axial ligand on the Al(porphyrin) monomer can afford Al-PPOPs with larger micropores that are more accessible to substrates in catalysis, the best catalysts are obtained after supercritical CO<sub>2</sub> processing. In contrast to the conventional activation method of heating the samples under vacuum, supercritical CO<sub>2</sub> processing affords POPs with much larger pores and total pore volumes, thus significantly enhancing substrate accessibility and catalytic rates. Supercritical CO<sub>2</sub> processing is also quite important in maintaining catalytic activity during the recycling. Together, these results indicate that supercritical processing can be an effective strategy to generate highly active reusable POP-based catalysts and suggest that it can be usefully deployed with other applications beyond catalysis where low-density, porous materials with very high total pore volumes are desired.

## ■ ASSOCIATED CONTENT

### 📄 Supporting Information

Synthesis procedures and characterization data. This material is available free of charge via the Internet at <http://pubs.acs.org>.

## ■ AUTHOR INFORMATION

### Corresponding Author

o-farha@northwestern.edu; j-hupp@northwestern.edu; stn@northwestern.edu

### Notes

The authors declare no competing financial interest.

## ■ ACKNOWLEDGMENTS

Financial support for this work is provided by DTRA (agreement HDTRA1-10-1-0023). Y.-S. K. thanks the Weinberg College of Arts and Sciences, Northwestern University for a Weinberg College summer 2011 research grant. Instruments in the Northwestern University Integrated Molecular Structure Education and Research Center (IMSERC) were purchased with grants from NSF-NSEC, NSF-MRSEC, Keck Foundation, the state of Illinois, and Northwestern University.

## ■ REFERENCES

- (1) Shultz, A. M.; Farha, O. K.; Hupp, J. T.; Nguyen, S. T. *J. Am. Chem. Soc.* **2009**, *131*, 4204.
- (2) Lee, D. H.; Kim, S.; Hyun, M. Y.; Hong, J.-Y.; Huh, S.; Kim, C.; Lee, S. J. *Chem. Commun.* **2012**, *48*, 5512.
- (3) Xie, M.-H.; Yang, X.-L.; Zou, C.; Wu, C.-D. *Inorg. Chem.* **2011**, *50*, 5318.
- (4) Lee, J.; Farha, O. K.; Roberts, J.; Scheidt, K. A.; Nguyen, S. T.; Hupp, J. T. *Chem. Soc. Rev.* **2009**, *38*, 1450.
- (5) Ma, L.; Abney, C.; Lin, W. *Chem. Soc. Rev.* **2009**, *38*, 1248.
- (6) Nagai, A.; Chen, X.; Feng, X.; Ding, X.; Guo, Z.; Jiang, D. *Angew. Chem., Int. Ed.* **2013**, *52*, 3770.
- (7) Ding, S.-Y.; Gao, J.; Wang, Q.; Zhang, Y.; Song, W.-G.; Su, C.-Y.; Wang, W. *J. Am. Chem. Soc.* **2011**, *133*, 19816.
- (8) McKeown, N. B.; Budd, P. M. *Chem. Soc. Rev.* **2006**, *35*, 675.
- (9) Mackintosh, H. J.; Budd, P. M.; McKeown, N. B. *J. Mater. Chem.* **2008**, *18*, 573.
- (10) Chen, L.; Yang, Y.; Jiang, D. *J. Am. Chem. Soc.* **2010**, *132*, 9138.
- (11) Jiang, J.-X.; Wang, C.; Laybourn, A.; Hasell, T.; Clowes, R.; Khimyak, Y. Z.; Xiao, J.; Higgins, S. J.; Adams, D. J.; Cooper, A. I. *Angew. Chem., Int. Ed.* **2011**, *50*, 1072.
- (12) Shultz, A. M.; Farha, O. K.; Hupp, J. T.; Nguyen, S. T. *Chem. Sci.* **2011**, *2*, 686.
- (13) Kaur, P.; Hupp, J. T.; Nguyen, S. T. *ACS Catal.* **2011**, *1*, 819.
- (14) Fraile, J. M.; García, J. I.; Mayoral, J. A. *Chem. Rev.* **2008**, *109*, 360.
- (15) Wang, C.; Zheng, M.; Lin, W. *J. Phys. Chem. Lett.* **2011**, *2*, 1701.
- (16) Zhang, Y.; Riduan, S. N. *Chem. Soc. Rev.* **2012**, *41*, 2083.
- (17) Whitesides, G. M.; Mathias, J. P.; Seto, C. T. *Science* **1991**, *254*, 1312.
- (18) Totten, R. K.; Ryan, P.; Kang, B.; Lee, S. J.; Broadbelt, L. J.; Snurr, R. Q.; Hupp, J. T.; Nguyen, S. T. *Chem. Commun.* **2012**, *48*, 4178.
- (19) Kang, B.; Kurutz, J. W.; Youm, K.-T.; Totten, R. K.; Hupp, J. T.; Nguyen, S. T. *Chem. Sci.* **2012**, *3*, 1938.
- (20) Morales-Rojas, H.; Moss, R. A. *Chem. Rev.* **2002**, *102*, 2497.
- (21) Dawson, R.; Cooper, A. I.; Adams, D. J. *Prog. Polym. Sci.* **2012**, *37*, 530.
- (22) Jiang, J.-X.; Su, F.; Trewin, A.; Wood, C. D.; Niu, H.; Jones, J. T. A.; Khimyak, Y. Z.; Cooper, A. I. *J. Am. Chem. Soc.* **2008**, *130*, 7710.
- (23) Weston, M. H.; Farha, O. K.; Hauser, B. G.; Hupp, J. T.; Nguyen, S. T. *Chem. Mater.* **2012**, *24*, 1292.
- (24) Weston, M. H.; Peterson, G. W.; Browe, M. A.; Jones, P.; Farha, O. K.; Hupp, J. T.; Nguyen, S. T. *Chem. Commun.* **2013**, *49*, 2995.
- (25) Wang, J.-L.; Wang, C.; deKrafft, K. E.; Lin, W. *ACS Catal.* **2012**, *2*, 417.
- (26) Ma, L.; Wanderley, M. M.; Lin, W. *ACS Catal.* **2011**, *1*, 691.
- (27) Totten, R. K.; Weston, M. H.; Park, J. K.; Farha, O. K.; Hupp, J. T.; Nguyen, S. T. *ACS Catal.* **2013**, *3*, 1454.
- (28) Nelson, A. P.; Farha, O. K.; Mulfort, K. L.; Hupp, J. T. *J. Am. Chem. Soc.* **2008**, *131*, 458.
- (29) Hüsing, N.; Schubert, U. *Angew. Chem., Int. Ed.* **1998**, *37*, 22.
- (30) Farha, O. K.; Yazaydin, A. Ö.; Eryazici, I.; Malliakas, C. D.; Hauser, B. G.; Kanatzidis, M. G.; Nguyen, S. T.; Snurr, R. Q.; Hupp, J. T. *Nature* **2010**, *2*, 944.

(31) Farha, O. K.; Eryazici, I.; Jeong, N. C.; Hauser, B. G.; Wilmer, C. E.; Sarjeant, A. A.; Snurr, R. Q.; Nguyen, S. T.; Yazaydin, A. Ö.; Hupp, J. T. *J. Am. Chem. Soc.* **2012**, *134*, 15016.

(32) Farha, O. K.; Wilmer, C. E.; Eryazici, I.; Hauser, B. G.; Parilla, P. A.; O'Neill, K.; Sarjeant, A. A.; Nguyen, S. T.; Snurr, R. Q.; Hupp, J. T. *J. Am. Chem. Soc.* **2012**, *134*, 9860.

(33) As a comparison, the initial per-Al(porphyrin) PNPDP methanolysis rate for <sup>scp</sup>Al-PPOP-2 is ~3 times faster than that for a homogeneous Al(porphyrin) dimer and ~9 times faster than an Al(porphyrin) tetramer; see refs 18 and 19.